Physica Medica 143 (2026) 105748

Contents lists available at ScienceDirect

Physica Medica

journal homepage: www.elsevier.com/locate/ejmp

Original paper

Personalized organ dose assessment from CT imaging during proton therapy for classical Hodgkin lymphoma patients☆

Angeliki Gkavonatsiou [a,b,*], Maite Romero-Expósito [a,c], Karin M Andersson [a,e], Mona Azizi [b,c], Christina Goldkuhl [d], Daniel Molin [e], Alexandru Dasu [a,e]

[a] The Skandion Clinic, Uppsala, Sweden
[b] Medical Radiation Physics, Stockholm University, Stockholm, Sweden
[c] Oncology Pathology Department, Karolinska Institutet, Stockholm, Sweden
[d] Department of Oncology, Sahlgrenska University Hospital, Gothenburg, Sweden
[e] Dept of Immunology, Genetics and Pathology, Uppsala University, Uppsala, Sweden

ARTICLE INFO

Keywords:
Imaging doses
Computed tomography
Hodgkin lymphoma
Personalized evaluation
Secondary doses
Proton therapy

ABSTRACT

Background/Purpose: Proton therapy (PT) improves treatment precision for classical Hodgkin lymphoma (cHL), with computed tomography (CT) being essential for treatment planning and verification. This study evaluates the individual organ doses from CT imaging in these patients treated with PT using free-breathing (FB) or deep inspirational breath hold (DIBH) techniques.

Material/Methods: A cohort of 38 patients treated at the Skandion Clinic was studied. Organ doses from each planning and verification scan were estimated using VirtualDose software, based on CT parameters extracted from DICOM data. The impact of different imaging protocols (standard dose [SD], low dose [LD], and 4DCT) was assessed for patients with target in mediastinum, and neck and upper thorax.

Results: Significant variations were observed in the number of CT scans (median 9, range 3–12) and the protocols used among patients. Organ doses were further influenced by the extent of the scanning volume and the scanning technique. SD protocols in the mediastinum set resulted in median dose per scan to the lungs around 21 mGy (males and females), while LD protocol reduced these doses by up to 87%. The most exposed organs can receive a total dose of several hundred mGy.

Conclusion: Large inter-patient variations highlight the need for personalized CT dose calculations. Although in-field and near-field organs may receive relatively high doses from imaging, these remain significantly lower than the prescribed dose, less than 2%. Nevertheless, organ doses and their associated risks for long-term survivors of cHL could be further minimized by implementing low-dose CT protocols whenever feasible.

1. Introduction

The general improvement in cancer patient survival rates means that the risk of radiation-induced long-term effects—such as cardiovascular diseases or radiation-induced second malignancies (RISM)—should be carefully considered during treatment planning [1], or at the very least, taken into account when communicating risks to patients and caregivers. Patients with classical Hodgkin lymphoma (cHL) represent a particular sensitive group when assessing the long-term effects of radiation. On the one hand, this disease has a very favourable prognosis, with up to 90% of patients at all stages being cured [2]. At the same time, a significant proportion of cHL cases occur in young patients, with 43% of cases affecting individuals under 34 years of age [https://seer.cancer.gov/statfacts/]. This combination of favourable prognosis and long-life expectancy increases the risk of developing late effects. In limited stages, treatment typically involves a short course of chemotherapy followed by radiotherapy. In cases where the mediastinum is involved, organs such as the heart, lungs, and breast may be compromised due to the received radiation dose.

Modern photon radiotherapy (RT) techniques, such as intensity-modulated radiotherapy (IMRT) and volumetric-modulated arc therapy (VMAT), create highly conformal dose distributions that reduce the

☆ This article is part of a special issue entitled: 'EURADOS and SINFONIA collaborations' published in Physica Medica.

* Corresponding author.
E-mail address: aggeliki.gkavonatsiou@gmail.com (A. Gkavonatsiou).

https://doi.org/10.1016/j.ejmp.2026.105748
Received 5 March 2025; Received in revised form 18 December 2025; Accepted 1 February 2026
Available online 5 February 2026

volume of treated tissues. However, this increased conformity comes at the cost of exposing larger volumes of normal tissue to low doses [3]. In this context, proton therapy (PT) offers an alternative. Due to its distinct physical characteristics, PT can deliver a lower dose outside the target volume, thereby reducing the integral dose to the patient's body. This tissue-sparing capability makes PT particularly advantageous for minimizing treatment-related complications [4]. However, the delivery of such highly conformal doses with sharp dose gradients between areas of high and low dose exposure necessitates high precision and accuracy, which can only be achieved through advanced image-guidance techniques [5,6].

Image-guided radiotherapy (IGRT) incorporates various imaging modalities at different stages of the treatment process, including planning, simulation, setup, and intrafraction monitoring [7]. Commonly used IGRT modalities include cone-beam computed tomography (CBCT), kilovoltage planar imaging, stereoscopic imaging, and portal imaging. These modalities enable precise verification of target structures before and, if necessary, during treatment, thus enhancing the accuracy of dose delivery achieved by advanced techniques. The trade-off, however, is that patients undergo more imaging procedures, leading to an increase in cumulative radiation exposure [8,9]. Rehani et al. [10] reported that 1.33% of patients undergoing CT scans accumulated effective doses greater than 100 mSv due to multiple imaging sessions, suggesting that numerous organs may have received doses exceeding this threshold. Therefore, a more detailed analysis of the dose range at the organ level is warranted.

At the Skandion Clinic, cHL patients are currently treated within a clinical trial studying, among other things, the clinical, dosimetric and physical conditions of pencil beam scanning (PBS) PT compared to the state-of-the-art photon therapy [https://cancercentrum.se/samverkan/vara-uppdrag/forskning/cancerstudier-i-sverige/studier/pro-hodgkin/]. One of the hypotheses of the trial is that PBS-PT results in fewer acute and late side effects, due to reduced dose delivered outside the target volume. A comprehensive analysis of the long-term effects, however, requires accounting for the imaging doses as well [11]. Thus, the purpose of this work was to evaluate the additional dose received by our cHL patients from CT scans acquired during planning and during verification of the treatment plan throughout the treatment course. The CT scans were performed in free-breathing (FB) or deep inspiration breath-hold (DIBH) and included scans using standard- dose (SD), low-dose (LD) and 4DCT protocols. The aim was to evaluate both the relative contributions of the different CT protocols and the absolute dose received by each patient over the entire course of their treatment.

2. Material and methods

The present study includes a cohort of 38 cHL patients (20 females, 18 males) who underwent PT at the Swedish PT center, the Skandion Clinic in Uppsala. In 26 cases, the target was in the mediastinum (Mediastinum set), while in the remaining cases, it involved lymph node regions located in the neck, supraclavicular fossae, or axillae (Neck and upper thorax set). The proton facility is run by the seven county councils with university hospitals and is based on a distributed competence concept. This means that immobilization, CT-scanning and treatment planning are performed at one of the university hospitals, while the treatment is given at the Skandion Clinic. The patients in this study were referred from one of the seven university hospitals.

The research methodology involves several key steps. The initial step entails the assessment and export of CT DICOM images for each patient from the Treatment Planning System (TPS), Eclipse v.16.1 (Varian Medical Systems, Inc), followed by categorization of the CT images based on the imaging protocol and the hospital of origin. The subsequent step involved extracting relevant metadata and calculating the CT organ doses. Each step of the methodology is elaborated in the following subsections.

2.1. Imaging protocols

Many cHL patients are treated in DIBH (for now on, RT-DIBH), especially with mediastinum involvement, since in addition to reduced target motion, healthy tissue can be spared due to the increased lung volume and a more beneficial position of the heart. The clinical workflow of the RT-DIBH patients at the Skandion Clinic has previously been described in detail [12,13].

The planning CT session is performed at one of the university hospitals in Sweden. For RT-DIBH, a CT scan without intravenous (IV) contrast agent is performed while a CT with IV contrast may also be conducted for more accurate target definition. Additionally, two extra CT scans in DIBH (for now on, CT-DIBH) are performed during the planning CT session to evaluate DIBH reproducibility. These CT-DIBH repetitions are most often performed with LD protocols. If the patient's condition prevents DIBH, the treatment is conducted in FB (for now on, RT-FB). In this case, a CT in FB (for now on, CT-FB) without IV contrast and a 4DCT including the target area with sufficient margins are performed during the planning CT session.

Except for one case, all patients in the Mediastinum set were treated with RT-DIBH. The neck and upper thorax set was treated with RT-FB. The treatment technique influences the imaging technique used; however, RT-DIBH patients may still undergo CT-FB scans, as shown in the results section.

A verification off-line CT scan is always performed at the proton clinic before the treatment start, including two additional LD CT scans for the RT-DIBH patients. Verifications CTs are then performed every week during the treatment course, or when considered necessary, with the option for adaptive re-planning. In each treatment fraction, planar kV imaging is used to ensure correct patient positioning.

In this study, CT series from the planning CT session together with all scans acquired during the treatment course have been included. PET-CT and CT series conducted before the CT planning session have not been included in the analysis. Moreover, since the dose contribution from planar imaging lies in the very low dose range [8] comparable to the calculation uncertainty of the CT, this contribution was not considered either.

2.2. Exportation and categorization of CT images

The CT image series were evaluated in the Eclipse system and categorized based on technique (CT-DIBH or CT-FB) and protocol (SD, LD or 4DCT). Additionally, the MOSAIQ health information system (Elekta Solutions AB) was used to further assess the number of CT images performed under each technique and protocol. After the assessment and categorization of the CT images, the CT series were exported.

2.3. VirtualDose calculations

The VirtualDose software [14] was used to calculate the organ doses. This is a user-friendly software based on Monte Carlo simulations, accessible online that requires to insert CT scan specific parameters (see Table 1) which can be obtained from the DICOM tags (Data used from the 4DCT scans were extracted from the averaged phase series). Once the appropriate parameters are inserted in the user interface, the software calculates the dose and reports organ doses in mGy.

2.3.1. Extraction of CT parameters

The parameters CT manufacturer and scanner model were obtained from either Eclipse or DICOM tags. The scan protocol was manually specified for each CT by checking the first and last slice position and the slice thickness using a DICOM viewer (3DSlicer [15] and MicroDicom DICOM Viewer [https://www.microdicom.com/]). The bowtie filter was chosen according to the DICOM tags regarding protocol and standard CTDI phantom. The beam collimation was chosen as 38.4 mm, 32 and 24 for CTs obtained by Siemens Definition AS+, Toshiba Aquilion/

Table 1
Parameters needed to be specified in VirtualDose.

Parameters	Option
Patient Phantom Type	The user can choose between various patient phantom types based on the Body Mass Index (BMI). The phantom types are described in more detail by Ding et al. [14].
Scan Protocol	Head, chest, abdomen-pelvis, chest-abdomen-pelvis, manually specified.
CT manufacturer	The user can choose between a variety of CT manufacturers.
Scanner model	The user can choose the desired scanner model of the CT manufacturer.
Bowtie filters	Body or head
Beam collimation (mm)	The user can choose between various values.
Peak kilovoltage (kVp)	The user can choose between various values.
Tube Current Modulation (TCM)	Yes or No
Exposure	The user inserts the value in mAs.*
Computed Tomography Dose Intex weighted (CTDIw) (per 100mAs)	The user inserts the value in mGy.*
Pitch	The user inserts the value.
Z-Over Scan Length (mm)	Yes or No (if Yes the user needs to specify the inferior and superior overcanning)

* If the value varies across the CT slices, the average value should be entered.

LB and Philips Brilliant Big Bore, respectively. The peak kilovoltage (kVp) as well as the use of the Tube Current Modulation (TCM) were found from the DICOM tags. The average exposure ($Exposure_{aver}$) of each CT scan was calculated by equation (1) using MATLAB (MathWorks, Inc):

$$Exposure_{aver}(mAs) = \frac{\sum_{i=1}^{N}(ExposureTime_i \times X - RayTubeCurrent_i)*1000}{N} \quad (1)$$

where, N is the total number of DICOM files, and $ExposureTime_i$ and $X - RayTubeCurrent_i$ are the values of the ith DICOM file (taken from the corresponding DICOM tag), respectively.

Typical pitch values of the CT series between the different manufacturers were 0.6, 0.8, and 0.09 when 4DCT was conducted. In the case of the CT series obtained by Siemens scans, the pitch value was calculated. For these scans it was found that the Exposure DICOM tag refers to the effective exposure which is equal to the exposure divided by the pitch. Based on this information the pitch value of Siemens CT scans was obtained by the following equation:

$$pitch = \frac{Exposure_{aver}}{Exposure_{eff,aver}} \quad (2)$$

Where $Exposure_{aver}$ is calculated by equation (1), and $Exposure_{eff,aver}$ is the effective average exposure, calculated from the DICOM tag as follows:

$$Exposure_{effaver} = \frac{\sum_{i=1}^{N} Exposure_i}{N} \quad (3)$$

where $Exposure_i$ is the exposure value of the ith DICOM file (taken by the corresponding DICOM tag).

The weighted Computed Tomography Dose Index ($CTDIw_{aver}$) (−per 100 mAs as required by the program) was obtained with equation (4) from the average value of the Volume Computed Tomography Dose Index ($CTDIvol_{aver}$), which was in turn calculated from the *CTDIvol* value of the ith DICOM file ($CTDIvol_i$), taken by the corresponding DICOM tag:

$$CTDI(per100mAs)_{w_{aver}} = CTDIvol_{aver} \times \text{pitch} \times \frac{100}{Exposure_{aver}} \quad (4)$$

$$CTDIvol_{aver} = \frac{\sum_{i=1}^{N} CTDIvol_i}{N} \quad (5)$$

$Exposure_{aver}$ and $CTDIvol_{aver}$ obtained from the DICOM tags using equation (1) and (5) were compared to the reported values from the CT scans in the Skandion Clinic for 3 patients, in a total of 14 CT scans.

The overscanning was examined in three patients by analysing their CT scan data. To calculate the overscan, the Dose Length Product (*DLP*) (product of *CTDIvol* and scan length), the *CTDIvol* and scan length are needed as follows:

$$overscan = \frac{DLP}{CTDIvol} - scanlength \quad (6)$$

The organ doses for each of the three patients' scans were calculated by inserting the overscanning values calculated by equation (6) (with half of the overscanning attributed to the inferior overscanning and the other half to the superior region of the scan). These results were then compared to the scenario without overscanning. In the rest of the patients of the study, no-overscanning option was applied.

To select the most accurate patient phantom, the body mass index (BMI) of the patient is required. However, weight and height information is not always available. For patients with sufficient data (a total of 10), the phantom was selected based on its BMI. For the others, the default adult male/female phantom was used. A dose comparison between using the appropriate BMI phantom and the reference adult phantom was conducted for an overweight patient to assess the impact of the phantom selection.

2.4. Analysis of organ doses

Doses to the following organs were analysed in this study: brain, thyroid, lungs, heart, breast, liver, stomach, colon, and gonads. First, the analysis of organ dose per single scan was conducted to compare the impact of different imaging protocols (CT-DIBH SD, CT-DIBH LD, CT-FB SD, and 4DCT). Subsequently, the total dose received was evaluated according to the specific number of scans per patient. Results for each data set (mediastinum or neck and upper thorax) and patient gender are presented in the following section.

3. Results

3.1. Organ doses per CT scan

Figs. 1 and 2 show the doses received by the heart and thyroid in each scan of representative patients from the mediastinum and the neck and upper thorax sets. One organ within the scanning region and another outside or at its border were selected. Accordingly, the heart was consistently within the scanning region for patients in the mediastinum set, whereas the thyroid was always within the field for patients in the neck and upper thorax set, with the opposite pattern observed for the other dataset. For each scan, the specific scanned region is shown, and details of the CT protocol and parameters are provided below the graphs.

From the mediastinum set, one RT-DIBH patient (left) and one RT-FB patient (right) are shown in Fig. 1. The RT-DIBH patient underwent 11 CT scans, while the RT-FB patient underwent 6 CT scans and 2 4DCT scans. In both cases, four distinct scan regions were identified. For a given organ, the absorbed dose was similar across scans of the same region when comparable exposure settings and $CTDIw_{aver}$ with the same scanner were applied (e.g. scans 5 and 6 in the RT-DIBH case). When higher exposure and $CTDIw_{aver}$ were applied, doses increased (e.g. scan 7 with the SD protocol compared with scans 8–11 with the LD protocol in the RT-DIBH patient). The effect of scan region size can be observed in the thyroid dose, which decreased from scan 2 (thyroid within the region) to scan 3 (thyroid outside). However, this effect may be masked by the protocol: for example, scans 3 and 4 (thyroid outside, SD protocol) yielded similar doses to scans 8–11 (thyroid inside, LD protocol). Protocol effects are also evident when comparing the RT-DIBH and RT-FB patients. The RT-FB patient predominantly underwent CT-FB and

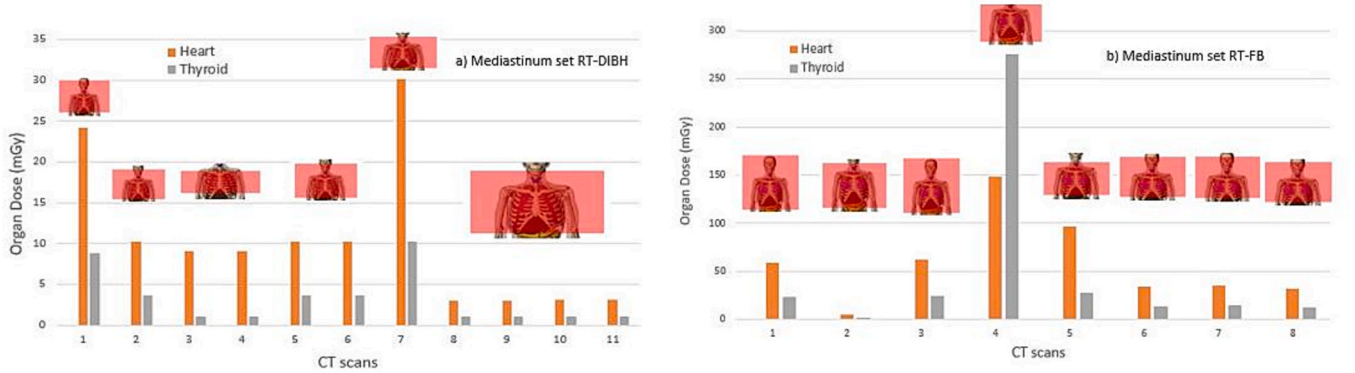

Scan	1	2	3	4	5	6	7	8	9	10	11
Dose protocol	SD	SD	SD	SD	SD	SD	SD	LD	LD	LD	LD
Exposure (mAs)	205.4	97.4	127.1	127.4	97.3	97.8	134.2	14.1	14.2	13.6	13.6
$CTDIw_{aver}$ (mGy)	9.7	4.6	6	6	4.6	4.6	11.1	1.2	1.2	1.1	1.1
Technique	DIBH	DIBH	DIBH	DIBH	FB	DIBH	DIBH	DIBH	DIBH	DIBH	DIBH
CTDI phantom	Body	Body	Body	Body	Body	Body	Body	Body	Body	Body	Body
Scanner	P#	P	P	P	P	P	S*	S	S	S	S

*S= Siemens Definition AS+ #P= Philips Big Bore

Scan	1	2	3	4	5	6	7	8
Dose protocol	SD	LD	SD	4DCT	4DCT	SD	SD	SD
Exposure (mAs)	97.6	13.4	106.1	75.0	89.6	128.3	124.7	118.1
$CTDIw_{aver}$(mGy)	16.7	1.6	17.6	9.8	5.9	10.6	10.3	9.8
Technique	DIBH	DIBH	FB	4DCT	4DCT	FB	FB	FB
CTDI phantom	Body	Body	Body	Body	Body	Body	Body	Body
Scanner	T#	T	T	T	S*	S	S	S

*S= Siemens Definition AS+ #T=Toshiba/Canon Aquilion LB

Fig. 1. Heart and thyroid doses of a RT-DIBH (left) and a RT-FB (right) from the mediastinum set. While the RT-DIBH patient received 11 CT scans, RT-FB patient received 8 CT scans. The scan range is illustrated on top of the corresponding CTs for both of the patients. The image of the scanning regions was taken by the output files of VirtualDose. Relevant data about imaging protocol, such as exposure and $CTDIw_{aver}$, from each CT is represented below the plot. The kVp value was 120 for all the scans.

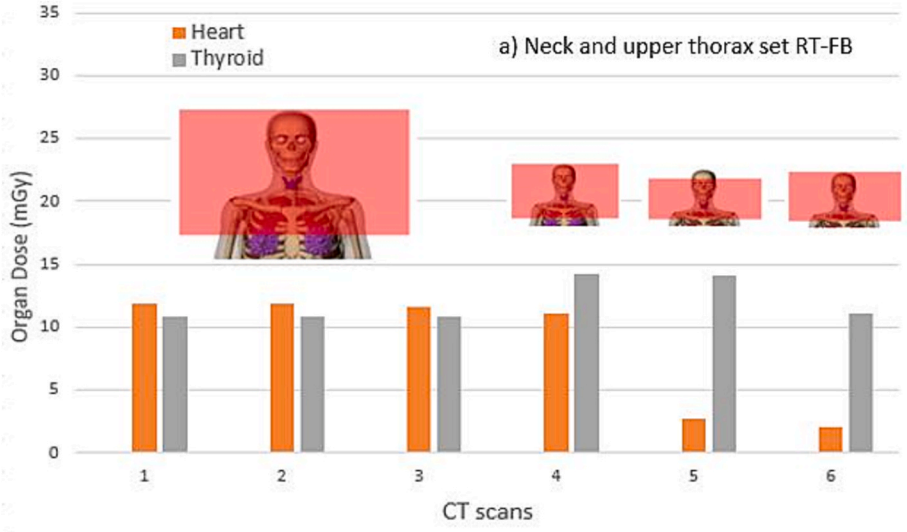

Scan	1	2	3	4	5	6
Dose protocol	SD	SD	SD	SD	SD	SD
Exposure (mAs)	105.2	105.2	104.5	78.9	72.4	51.2
$CTDIw_{aver}$ (mGy)	7.1	7.1	7	6.5	6	4.2
Technique	FB	FB	FB	FB	FB	FB
CTDI phantom	Body	Body	Body	Body	Body	Body
Scanner	S*	S	S	S	S	S

*S= Siemens Definition AS+

Fig. 2. Heart and thyroid doses of a RT-FB patient from the neck and upper thorax set, that received 8 CT scans. The scan range is illustrated on top of the corresponding CTs for the patient. The image of the scanning regions was taken by the output files of VirtualDose. Relevant data about imaging protocol, such as exposure and $CTDIw_{aver}$, from each CT is represented below the plot. The kVp value was 120 for all the scans.

4DCT scans using SD protocols, resulting in higher doses. Nevertheless, differences in scanner models and other parameters are expected to also influence the results.

Fig. 2 shows an RT-FB patient from the neck and upper thorax set. Comparing the patients from the two different sets, mediastinum, and neck and upper thorax, the scanning regions differ considerably. The scans in patients from the mediastinum set include mainly the whole thorax and/or abdomen while in most of the patients from the neck and

upper thorax set, only the head and upper thorax are inside the scanning area. For the RT-FB patient in Fig. 2, scans 4–6 show a higher dose in thyroid compared to the heart, likely due to the scanning region covering a smaller portion of the heart than in scans 1–3.

Figs. 3 to 6 show a more detailed analysis of the effect of CT protocol on organ doses for the two patient sets. The analysis includes organs located within the primary irradiated region and those positioned outside the scanning area. In general, it is noticed in all figures that organs located closer to the primary irradiated region, such as lungs, heart and breast, received higher doses (about few tens of mGy). In contrast, organs located further from the scanning region, such as gonads, which were consistently outside the scanning field, received substantially lower doses (well below 1 mGy).

Fig. 3 illustrates a comparison of organ doses across different CT protocols for male patients (11) from the mediastinum set including 45 scans in SD (left), 72 scans in LD (centre) and two 4DCT scans (right). As expected, SD resulted in higher median doses across most organs compared to LD protocols, reflecting the objective of LD protocols to minimize radiation exposure while maintaining acceptable image quality. Specifically, median doses for SD protocols were 20.8 mGy and 17.3 mGy in lungs and breast, respectively, whereas the corresponding median doses for LD protocols were 3.4 mGy and 2.8 mGy, respectively, indicating an approximately 83% dose reduction. The highest doses, however, were observed for 4DCT scans, with median values of 34.4 mGy to the lungs and 33.7 mGy to the breast. It should be noted that the median values of 4DCT doses have lower significance due to the low number of scans been performed.

A rough quantification of dose variability within each organ for the same protocol was obtained by calculating the interquartile range over the median organ dose. In the male mediastinum set, lung dose variability was 42% for LD protocols compared with 81% for SD protocols. This higher variability in SD protocols may indicate less consistency in scanning parameters and set-ups across clinics. In fact, the scattered points observed in LD protocols correspond to CT scans acquired with higher exposure and CTDIvol than most LD protocols in the study. As shown in Figs. 1 and 2, differences in scanned region and manufacturer may also contribute to this variability.

Fig. 4 presents the organ doses for male patients (six) from the neck and upper thorax set including 24 scans, all conducted with SD protocol. Compared with SD scans from the mediastinum set, median total doses were lower, for example the median lung dose was 11.5 mGy, with lower variability (69%), while the median breast dose was 10.39 mGy with higher variability (118% vs. 81%). The outliers in Fig. 4 correspond to

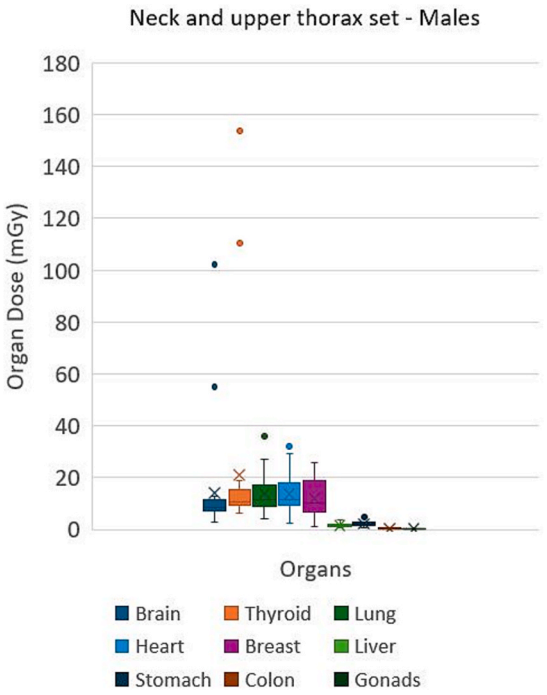

Fig. 4. Dose distribution in male patients from the neck and upper thorax set per CT scan with SD protocol (36 scans) among different organs. The cross symbol indicates the mean, while the horizontal line represents the median.

two scans conducted without TCM: one scan in an obese patient and one in a standard patient. These resulted in increased organ doses, particularly in brain and thyroid, in comparison with the rest of the scans where TCM was activated.

Similar variabilities were observed in organ doses across the different techniques for organs never included in the scanning region. However, this is of much lower concern since the absolute doses are considerably lower. For example, the median dose in gonads is equal to 0.1 mGy, 0.4 mGy and 0.06 mGy in CT scans from the neck and upper thorax set, the mediastinum set with SD, and LD protocol, respectively.

Consistent behaviour was observed in female patients, as depicted in Fig. 5 (mediastinum set scans: 50 SD, 88 LD, five 4DCT) and Fig. 6 (neck and upper thorax set: 22 scans at SD). The median dose in neck and

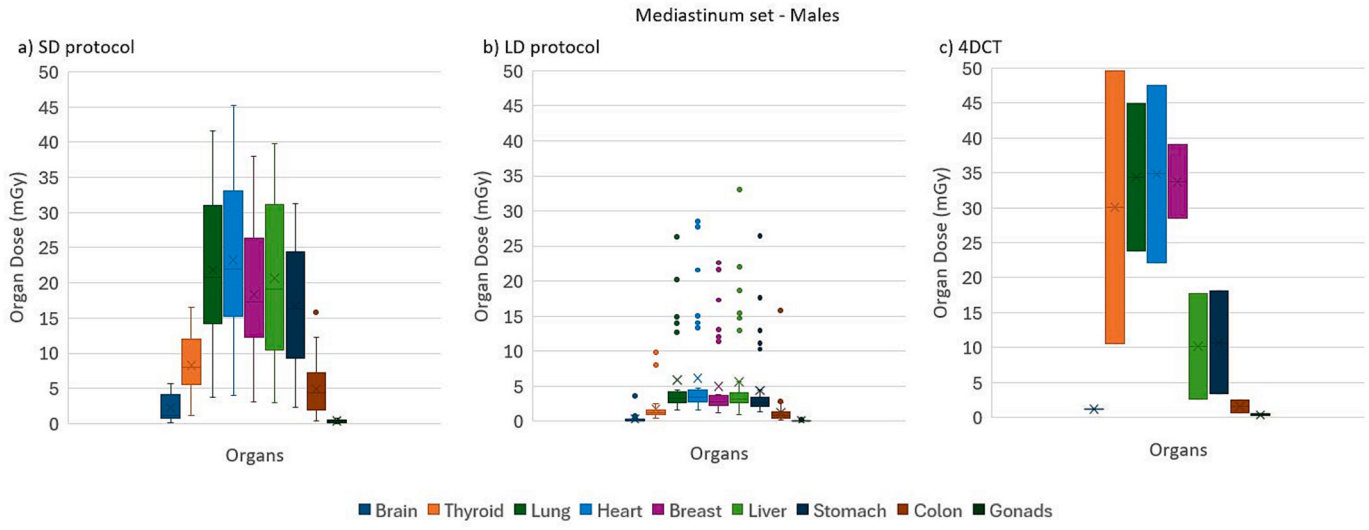

Fig. 3. Dose distribution in male patients from the mediastinum set per CT scan with SD protocol (33 scans) (left), LD protocol (76 scans) (centre), and 4DCT (two scans) (right) among different organs. The cross symbol indicates the mean, while the horizontal line represents the median.

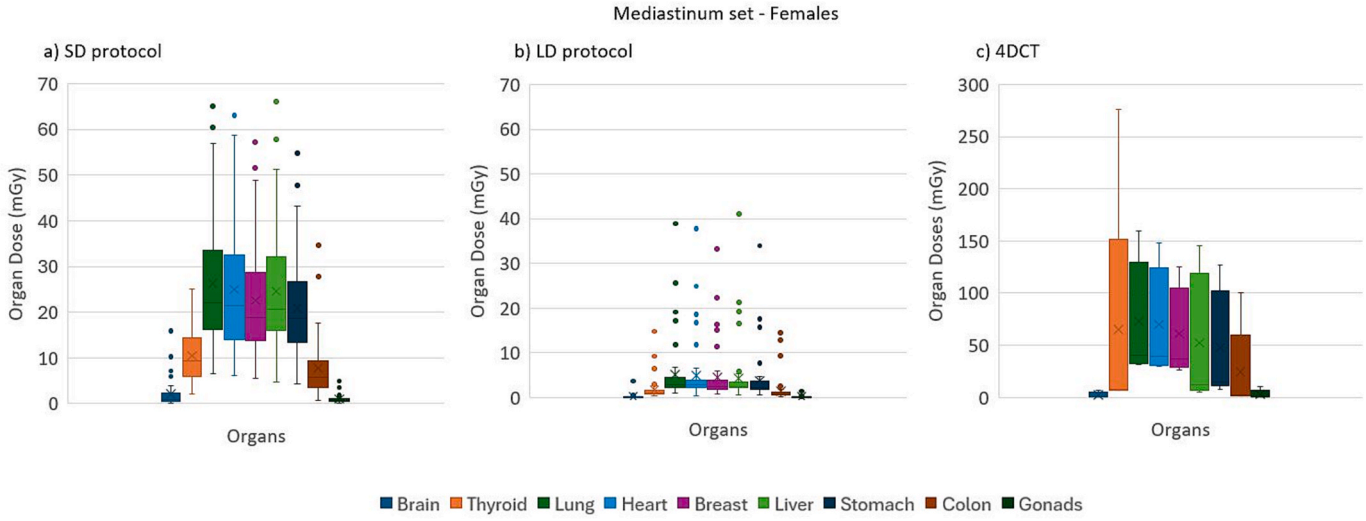

Fig. 5. Dose distribution in female patients from the mediastinum set per CT scan with SD protocol (36 scans) (left), LD protocol (80 scans) (centre), and 4DCT (five scans) (right) among different organs. The cross symbol indicates the mean, while the horizontal line represents the median.

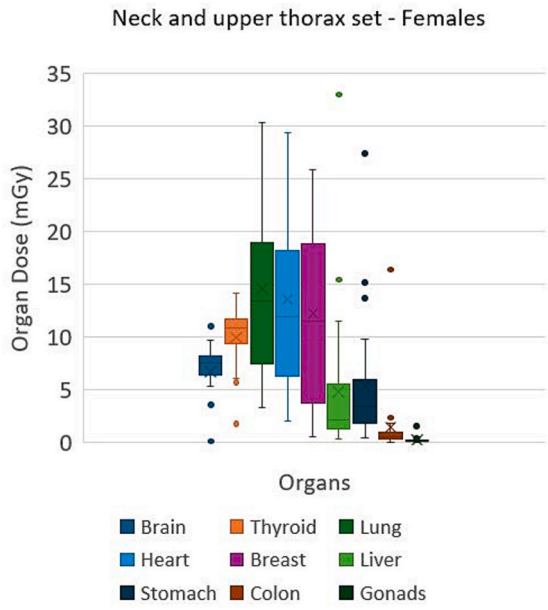

Fig. 6. Dose distribution in female patients from the neck and upper thorax set per CT scan (34) among different organs. The cross symbol indicates the mean, while the horizontal line represents the median.

upper thorax scans was 13.4 mGy in lungs, 11.5 mGy in breast and 0.2 mGy in gonads, while the median dose of scans with LD protocol from the mediastinum set in lungs was 3.4 mGy, 2.9 mGy in breast and 0.1 mGy in gonads, and scans with SD protocol resulted in median dose of 22.1 mGy in lungs, 18.9 mGy in breast and 0.7 mGy in gonads. Higher values were obtained for the 4DCT scans inside the scanning area with 40.7 mGy in lungs and 39.5 mGy in heart, but 0.5 mGy in gonads. Once again, these 4DCT values should be interpreted with caution due to the low number of scans. The maximum dose value in lungs in the scans from the neck and upper thorax set, mediastinum set with LD and SD protocol could reach up to 30.34 mGy, 38.91 mGy and 65.1 mGy, respectively. The variability in LD scans from the mediastinum set was similar to that with SD protocol, with 78% versus 76% in the lungs and breast.

Similar to the case of male patients, the scattered points of LD protocols in Fig. 5 (centre) correspond to CT scans with higher exposure and CTDIvol, while in the case of SD protocols, and scans of neck and upper thorax set (Fig. 6), the scattered points indicate differences in the scanning area, where some scans did not include the brain and/or some scans included part of the abdomen.

In addition to the effect of imaging protocol, we also studied the effect of overscanning and patient size. Using Equation (6), overscanning calculations for the three patients indicated variations in organ doses from 0% to 4% when comparing scenarios with and without overscanning. However, this is important for organs that are in the borders of the scanning region. For instance, for one patient, the overscanning scenario led to significantly elevated organ doses, with breast doses increasing by up to 183% and heart doses by up to 74%. More specifically, the dose to breast increased from 5.4 mGy to 15.2 mGy and to the heart from 6.6 mGy to 11.6 mGy after including the overscanning. In comparison, the dose to the thyroid increased from 9.2 mGy to 9.5 mGy, leading to an increase of only 3.5%.

The comparison between organ doses using the overweight patient phantom and the default adult phantom showed a difference in total organ dose that ranges from 2% to 50%. More particularly, the thyroid and the brain, which were located within the scanning region, experienced a 13% and 25% decrease in dose respectively, when the overweight phantom was applied. However, for organs partially included in the scanning region contradictory results were obtained. For example, while the breast dose is higher in the smaller phantom, lung and heart doses were lower.

Finally, we tested the effect of using data extracted from the DICOM tags or data from the scan reports, which in some instances were found to be different. The comparison revealed differences ranging from 0.1% to 6.8% in exposure and from 0.1% to 3.1% in CTDIvol.

3.2. *Total organ dose per patient*

Fig. 7 presents the total CT doses per RT-DIBH patient from the mediastinum set (25 patients, left) and the one RT-FB patient from the mediastinum set (right) over the entire RT course. Fig. 8 shows the total CT doses for RT-FB patients from neck and upper thorax set. The median value of total CT dose in RT-DIBH patients to lungs and heart, which are always included in the scanning region, is equal to 131.4 mGy and 129.6 mGy, respectively. In RT-FB patients from the neck and upper thorax set, where these organs are not always inside the scanning region, the doses reduced to 59.8 mGy and 53.1 mGy, respectively. By contrast, brain is most often within the scanning region in RT-FB patients from the neck and upper thorax set, leading to higher doses compared to RT-FB

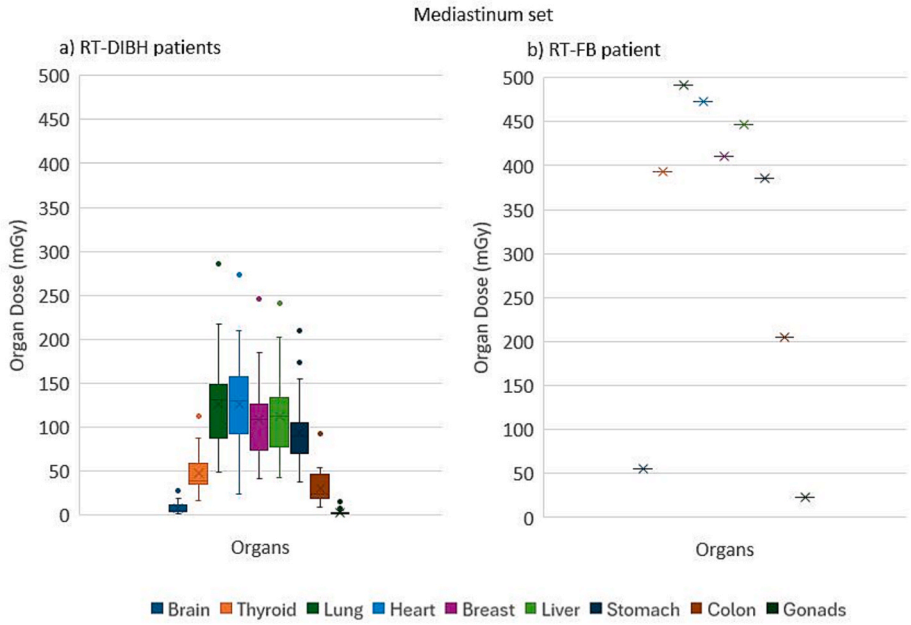

Fig. 7. Total CT dose distribution among different organs in patients from the mediastinum set with RT-DIBH (left) and one patient from the mediastinum set with RT-FB (right). The cross symbol indicates the mean, while the horizontal line represents the median.

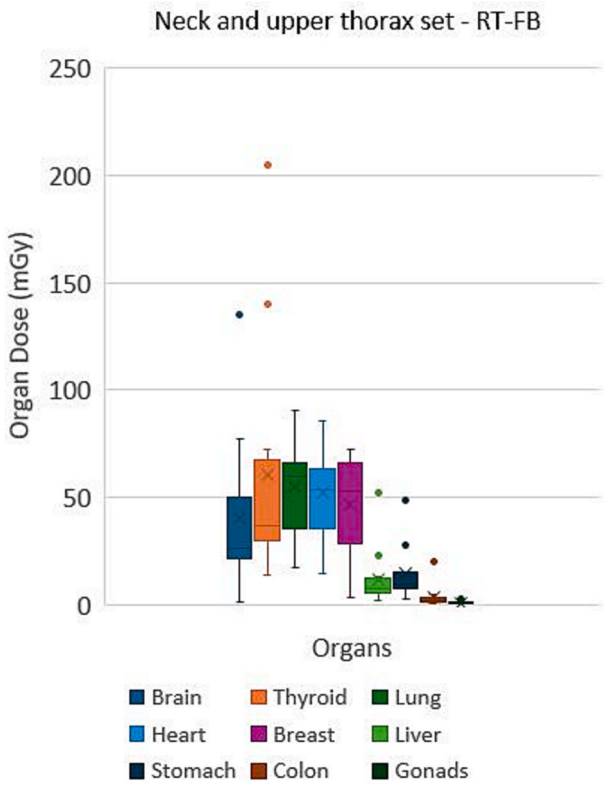

Fig. 8. Total CT dose distribution among different organs in patients from the neck and upper thorax set with RT-FB. The cross symbol indicates the mean, while the horizontal line represents the median.

patients from the mediastinum set (26.4 mGy vs. 5.1 mGy). The median total CT dose to the gonads is significantly lower in both cases, 2.4 mGy in patients from the mediastinum set and 0.6 mGy in the neck and upper thorax set.

When comparing the median total organ doses of RT-DIBH patients with those of the single RT-FB patient (Fig. 7), the RT-FB patient showed higher exposures, exceeding 350 mGy in six organs. As shown in Fig. 1 (right), this patient underwent predominantly SD CT scans and two 4DCT scans, which contributed to the increased total organ doses. As a reference, the median dose in lung increased from 131 to 492 mGy.

The variability in organ doses among patients from the mediastinum set, and the neck and upper thorax set, as presented in Section 3.2, can also be observed in the scatter points, indicating differences in scanning regions and the number of CT performed under different protocols (SD, LD, 4DCT) between the patients. While most patients from the neck and upper thorax set undergo CT scans covering head and upper thorax (see Section 3.1), some cases include whole thorax and part of the abdomen in the scanning region contributing to dose fluctuations especially on liver, stomach and colon as it is shown at the scattered points in Fig. 8. The scattered points on brain and thyroid in Fig. 8 correspond to two patients (one obese, one standard size) where some CT scans were conducted with TCM off, increasing the received total organ dose.

Additionally, the number of CT scans performed per patient plays a role. Across the entire patient group, the number of scans ranged from 3 to 12. Mediastinum RT-DIBH patients underwent a median of 10 scans (including a median of 2 SD and 5 LD protocols in CT-DIBH series, and 1 CT-FB series), whereas the median number for head and upper thorax patients was 4. This lower number of scans further contributes to the decrease in total dose when comparing the groups.

4. Discussion

To our knowledge, this is the first systematic analysis of the imaging doses in cHL patients treated with PT, evaluating CT doses for all scans acquired during the RT course while accounting for the specific parameters of each scan. We focused on organ doses rather than effective dose. While effective dose is useful for comparing exposure scenarios, it is not intended for individual risk assessment [16]. The ultimate goal of our study is precisely to contribute to such individual assessments by combining these imaging-related doses with those received from radiotherapy, thus providing better insight into potential long-term effects [11].

CHL patients may undergo CT and PET-CT scans prior to the treatment course, as well as planar kilovoltage imaging during treatment. Since it is recommended to account for all imaging doses when

estimating total patient exposure for a more precise evaluation, the absence of these data represents a limitation of our study. However, in the case of planar imaging, the contribution is minimal. Hälg et al. [8] reported that planar kilovoltage images result in an additional dose of less than 0.5% of the prescribed dose. For example, depending on the imaging protocol, lung and heart doses ranged between 0.0002 and 0.005 mGy [8].

As expected, our analysis showed that organs that are included partially or entirely inside the scanning region, such as lungs, heart, breast, thyroid and liver, receive higher doses than organs that are never included, such as gonads. In the mediastinum set, a patient undergoing a RT-DIBH course could receive doses up to 300 mGy due to the required CT scans, compared with nearly 500 mGy for a RT-FB course. However, the number of patients in our datasets is insufficient to provide reference values, particularly for the RT-FB protocol, which was followed by only one patient. In contrast, the high interpatient variability in the number and types of scans, as well as intrapatient variability in scanning parameters (exposure and $CTDIw_{aver}$) and scanning region (as seen in Figs. 1-2), could be representative of a cHL population. These variations result in large differences in the organ doses and highlight the importance of personalized dose calculations for imaging assessments. In this sense the use of more accurate input data, results in more accurate results.

In this work, organ doses were calculated using the VirtualDose software. This tool employed a precalculated organ dose database, obtained by MC simulations, to perform rapid dose estimations for several scanner manufacturers and models [14]. The number of photons used in their simulations ensure relative errors lower than 1% for organs near the primary beam and 5% for those located in larger distances or with very small volumes. The database is then adjusted by the CT parameters of the particular scan and scanner to provide the organ doses in the patient. Parameters such as exposure, CTDw, kVp and pitch were extracted from the DICOM tags of each data series. A study by De Mattia et al. [17] showed that VirtualDose results are more sensitive to changes on the tube voltage and CTDIvol compared to other exposure parameters. Moreover, the program relies on fixed values for exposure and CTDIw for the calculation, rather than using slice-specific values, which would provide the most accurate results. As explained in Section 2.3.1, average values were calculated and inserted in the VirtualDose interface. The program handles these values differently depending on whether TCM is activated. When TCM is not applied, exposure and CTDIw are considered constant throughout the CT acquisition, whereas when TCM is activated, the values are treated as averages. The impact and modelling of TCM was studied by Tian et al. (2015) [18], showing that for a chest scan, average organ doses decreased by up to 43% for the heart and 25% for the lungs in scans with high modulation compared to scans without modulation. In our datasets, many of the outliers were attributable to the absence of TCM during acquisition.

One of the most critical parameters in the evaluation of organ doses is patient anatomy, which is the basis for a personalized approach. VirtualDose includes a set of 25 realistic voxel phantoms covering the 50th percentile of the different type of phantoms (for more information about the phantom types see Ding et al. [14]), to cover the needs of specific patient size. It has been compared to other software that use more simplified anatomies based on stylized phantoms [14] resulting in more accurate results related to anatomical realistic geometries. To choose the right phantom size based on the patient size, the BMI value is required. However, in the current study the height was not recorded for all the patients highlighting the need of more detailed patient specific information. Comparison between the default adult phantom and an overweight phantom keeping the rest parameters the same, illustrated that organs inside the scanning region received higher radiation dose with the smaller phantom. These results agree with the results of Ding et al. [14], where it is mentioned that smaller patient phantom receives higher radiation doses especially for those located inside the scanning region. However, this was not observed in all organs partially included in the scanning region. As it has been discussed by De Mattia et al. [17] the organs at the border of the scanning region are more affected by changes in the phantom type, where the scatter contribution is more relevant. Given that dose differences can be as high as 50%, recording the patient's height and weight is strongly recommended when using dose calculation tools based on predefined phantoms. Nevertheless, even when selecting the most appropriate phantom in terms of size and gender, anatomical differences between the actual patient and the reference healthy phantom increase the uncertainty of the calculated dose. These discrepancies may be further accentuated in DIBH scans due to the increased thoracic volume. Ideally, the most accurate results would be obtained by using the patient's actual anatomy—namely, their CT images—for the calculation. However, this approach would require Monte Carlo simulations, which are impractical for routine clinical use. Although this limitation may affect the dose values, the partial personalization in this study is preserved by using the specific scanning parameters of each individual scan—including the actual scanning range—rather than relying on default protocols for major anatomical regions (head and neck, thorax/abdomen).

Our study has shown that DICOM tags – which could enable implementing automated solutions for the calculation – may differ from the values reported from scan acquisition. However, the impact of these discrepancies was low and within the uncertainties of the calculation. In the case of the overscanning, the critical scenario is when the organ is located on the border of the scanned region. Here the increase of few mm has a high impact on the dose, which has been also observed by De Mattia et al. [17]. In our study, one patient had a significative increase in the dose, up to 183% in breast and 74% in heart (see section 3.1). However, even though the increase is significantly high, the absolute doses remain low after the overscanning. The determination of the overscanning value was not feasible through the DICOM tags alone, therefore the method described in Section 2.3.1 was implemented to estimate this parameter and evaluate its influence on organ doses. The method detailed in equation (6), necessitates patient specific scanning information which may not always be accessible in the hospital's record. Furthermore, even when the data are available, the process of retrieving and analysing is labour-intensive and susceptible to errors, potentially introducing deviations in the results.

Addressing the methodological limitations discussed could improve the accuracy of the doses received by our patients due to the CT scans acquired during their RT treatment. However, the order of magnitude and the observed differences are sufficient to draw valid conclusions regarding the use of CT as a verification system in PT. In particular, the repeated CT scans are important to verify anatomical variations of the patient during the treatment to allow the safe delivery of the therapeutic doses to the target while sparing the organ at risk. According the AAPM TG-180 [19], the dose from repeated imaging procedures should be considered part of the total dose at planning stage if is expected to exceed 5% of the prescribed target dose. For the 38 patients included in the study the prescribed dose ranged between 20 and 29.7 Gy_{RBE} and the total CT organ doses were below this 5% threshold. Namely, lung and heart doses were between 0.2% and 1% of the prescribed dose in the mediastinum set treated with DIBH. For the single FB patient, who received the highest doses, the values remained below 2%. In the neck and upper thorax set, thyroid doses were below 1%. However, different results may be obtained when comparing to the actual dose received by the organ during the RT treatment. For example, the CT dose to the lungs in patients with mediastinum involvement is on average 2% of the dose received directly from the RT treatment [20].

The small contribution from the CT scans reduces concern about their repeated use, especially compared to the high anatomical precision they provide. However, for patients undergoing a high number of scans, particularly those treated in DIBH, a LD protocol was implemented for most of the repetitions. In our institution, using a Siemens scanner, the LD protocol primarily involved reducing the exposure and CTDIw by up to one order of magnitude (a decrease of 80–90%), while maintaining

the same kVp and pitch. Another institution, using a Philips scanner, relied on reducing the kVp from 120 to 90. Since no standardised protocols exit, each facility adapts according to its own resources. Importantly, our results indicate that LD implementation can reduce doses by up to 83% through optimisation of scan parameters. Therefore, it is essential the use of the LD protocols whenever possible to minimize the organ doses and, consequently, their associated risks. Nevertheless, in cancer treatment it is important to prioritise the delivery of the therapeutic dose to the target to ensure the long-term survival of the patient.

5. Conclusion

During the course of PT, it is crucial to verify the position and anatomy of the patient to ensure healthy tissue sparing. Therefore, repeated CT scans may be used with different protocols and techniques, such as SD/LD, FB/DIBH, and 4DCT, depending on the individual patient's treatment needs. However, CT scans contribute to additional radiation exposure for patients undergoing PT.

The results of this study demonstrated the large variation that could be expected in organ doses depending on the number of scans and scanning parameters, such as exposure settings and scanning region. Organs located within or near the scanning region received higher doses compared to those positioned further away. Scans including whole thorax/abdomen performed with LD protocol resulted in lower organ doses compared to the SD protocol and head/upper thorax scans. The influence of CT and patient-specific parameters on organ dose highlights the importance of individualized dose calculations. In particular, recording patient information such as height and weight proved to be important.

Although the contribution of CT scans to organ doses is relatively minor compared to the prescribed PT dose, low-dose protocols should be applied to minimize potential long-term risks, especially for the sensitive population of cHL patients.

Declaration of competing interest

The authors declare that they have no known competing financial interests or personal relationships that could have appeared to influence the work reported in this paper.

Acknowledgments

This project has received funding from Euratom's research and innovation programme 2019-20 under grant agreement no. 945196.

References

[1] Newhauser WD, de Gonzalez AB, Schulte R, Lee C. A review of radiotherapy-induced late effects research after advanced technology treatments. Front Oncol 2016;6:13. https://doi.org/10.3389/fonc.2016.00013.

[2] Brice P, de Kerviler E, Friedberg JW. Classical Hodgkin lymphoma. Lancet 2021 Oct 23;398(10310):1518–27. https://doi.org/10.1016/S0140-6736(20)32207-8. Epub 2021 Jan 22 PMID: 33493434.

[3] Hoppe BS, et al. Effective dose reduction to cardiac structures using protons compared with 3DCRT and IMRT in mediastinal Hodgkin lymphoma. Int J Radiat Oncol Biol Phys Oct. 2012;84(2):449–55. https://doi.org/10.1016/j.ijrobp.2011.12.034.

[4] Newhauser WD, Zhang R. The physics of proton therapy. Phys Med Biol. 2015 Apr 21;60(8):R155-209. doi: 10.1088/0031-9155/60/8/R155. Epub 2015 Mar 24. PMID: 25803097; PMCID: PMC4407514.

[5] Lane S, Slater J, Yang G. Image-guided proton therapy: A comprehensive review. Cancers 2023;15:2555. https://doi.org/10.3390/cancers15092555.

[6] Bolsi A, Peroni M, Amelio D, Dasu A, Stock M, Toma-Dasu I, et al. Practice patterns of image guided particle therapy in Europe: A 2016 survey of the European Particle Therapy Network (EPTN). Radiother Oncol 2018 Jul;128(1):4–8. https://doi.org/10.1016/j.radonc.2018.03.017. Epub 2018 Mar 28 PMID: 29605478.

[7] Murphy MJ, Balter J, Balter S, BenComo JA, Das IJ, Jiang SB, et al. The management of imaging dose during image-guided radiotherapy: Report of the AAPM Task Group 75. Med Phys 2007;34(10):4041–63. https://doi.org/10.1118/1.2775667.

[8] Hälg RA, Besserer J, Schneider U. Systematic measurements of whole-body imaging dose distributions in image-guided radiation therapy. Med Phys 2012;39(12):7650–61. https://doi.org/10.1118/1.4758065.

[9] Gudowska I, Ardenfors O, Toma-Dasu I, Dasu A. Radiation burden from secondary doses to patients undergoing radiation therapy with photons and light ions and radiation doses from imaging modalities. Radiat Prot Dosim 2014 Oct;161(1–4):357–62. https://doi.org/10.1093/rpd/nct335. Epub 2013 Dec 18 PMID: 24353029.

[10] Rehani MM, Yang K, Melick ER, Heil J, Šalát D, Sensakovic WF, et al. Patients undergoing recurrent CT scans: Assessing the magnitude. Eur Radiol 2020;30(4):1828–36. https://doi.org/10.1007/s00330-019-06523-y.

[11] Romero-Expósito M, Sánchez-Nieto B, Riveira-Martin M, Azizi M, Gkavonatsiou A, Muñoz I, et al. Individualized evaluation of the total dose received by radiotherapy patients: Integrating in-field, out-of-field, and imaging doses. Phys Med 2025;129:104879. https://doi.org/10.1016/j.ejmp.2024.104879.

[12] Andersson KM, Edvardsson A, Hall A, Enmark M, Kristensen I. Pencil beam scanning proton therapy of Hodgkin's lymphoma in deep inspiration breath-hold: A case series report. Tech Innov Patient Support Radiat Oncol 2019 Dec;23(13):6–10. https://doi.org/10.1016/j.tipsro.2019.11.006. PMID: 32128456; PMCID: PMC7042155.

[13] Hörberger F, Andersson KM, Enmark M, Kristensen I, Flejmer A, Edvardsson A. Pencil beam scanning proton therapy for mediastinal lymphomas in deep inspiration breath-hold: A retrospective assessment of plan robustness. Acta Oncol 2024 Feb;28(63):62–9. https://doi.org/10.2340/1651-226X.2024.23964. PMID: 38415848; PMCID: PMC11332452.

[14] Ding A, Gao Y, Liu H, Caracappa PF, Long DJ, Bolch WE, et al. VirtualDose: A software for reporting organ doses from CT for adult and pediatric patients. Phys Med Biol 2015 Jul 21;60(14):5601–25. https://doi.org/10.1088/0031-9155/60/14/5601. Epub 2015 Jul 2 PMID: 26134511.

[15] Fedorov A., Beichel R., Kalpathy-Cramer J., Finet J., Fillion-Robin J-C., Pujol S., Bauer C., Jennings D., Fennessy F., Sonka M., Buatti J., Aylward S.R., Miller J.V., Pieper S., Kikinis R. 3D Slicer as an Image Computing Platform for the Quantitative Imaging Network. Magnetic Resonance Imaging. 2012 Nov;30(9):1323-41. PMID: 22770690. (http://www.slicer.org).

[16] Icrp. The 2007 recommendations of the international commission on radiological protection. ICRP Publication 103. Ann ICRP 2007;37(2–4).

[17] De Mattia C, Campanaro F, Rottoli F, Colombo PE, Pola A, Vanzulli A, et al. Patient organ and effective dose estimation in CT: comparison of four software applications. Eur Radiol Exp 2020 Feb 14;4(1):14. https://doi.org/10.1186/s41747-019-0130-5. PMID: 32060664; PMCID: PMC7021892.

[18] Tian X, Li X, Segars WP, Frush DP, Samei E. Prospective estimation of organ dose in CT under tube current modulation. Med Phys 2015;42:1575–85. https://doi.org/10.1118/1.4907955.

[19] Ding GX, Alaei P, Curran B, Flynn R, Gossman M, Mackieet TR, et al. Image guidance doses delivered during radiotherapy: Quantification, management, and reduction: Report of the AAPM therapy physics committee task group 180. Med Phys 2018;45(5):e84–99. https://doi.org/10.1002/mp.12824.

[20] Romero-Expósito M, Gkavonatsiou A, Azizi M, Norrlid O, Goldkuhl C, Molin D, et al. SC34.03 contribution of ct scans to total dose received by proton radiotherapy patients. analysis on a classical hodgkin lymphoma cohort. Phys Med 2024;125S1:103552. https://doi.org/10.1016/j.ejmp.2024.103552.